THE JOURNAL OF BIOLOGICAL CHEMISTRY
Vol. 276, No. 33, Issue of August 17, pp. 30834–30844, 2001

Printed in U.S.A.

Epitope Diversity of *N*-Glycans from Bovine Peripheral Myelin Glycoprotein P0 Revealed by Mass Spectrometry and Nano Probe Magic Angle Spinning ^{1}H NMR Spectroscopy*

Received for publication, February 2, 2001, and in revised form, June 6, 2001
Published, JBC Papers in Press, June 15, 2001, DOI 10.1074/jbc.M101013200

Ricardo Gutiérrez Gallego‡§, José L. Jiménez Blanco‡§¶, Carol W. E. M. Thijssen-van Zuylen‡, Charlotte H. Gotfredsen‖, Hans Voshol‡‡, Jens Ø. Duus‖, Melitta Schachner‡‡, and Johannes F. G. Vliegenthart‡§§**

From the ‡Bijvoet Center, Department of Bio-organic Chemistry, Utrecht University, NL-3508 TB Utrecht, The Netherlands, the ‡‡Department of Neurobiology, Swiss Federal Institute of Technology, Höggerberg, CH-8093 Zürich, Switzerland, and the ‖Department of Chemistry, Carlsberg Laboratory, Gamle Carlsberg Vej 10, DK-2500 Valby, Copenhagen, Denmark

The carbohydrate structures present on the glycoproteins in the central and peripheral nerve systems are essential in many cell adhesion processes. The P0 glycoprotein, expressed by myelinating Schwann cells, plays an important role during the formation and maintenance of myelin, and it is the most abundant constituent of myelin. Using monoclonal antibodies, the homophilic binding of the P0 glycoprotein was shown to be mediated via the human natural keller cell (HNK)-1 epitope (3-*O*-SO_3H-GlcUA(β1–3)Gal(β1–4)GlcNAc) present on the *N*-glycans. We recently described the structure of the *N*-glycan carrying the HNK-1 epitope, present on bovine peripheral myelin P0 (Voshol, H., van Zuylen, C. W. E. M., Orberger, G., Vliegenthart, J. F. G., and Schachner, M. (1996) *J. Biol. Chem.* 271, 22957–22960). In this study, we report on the structural characterization of the detectable glycoforms, present on the single *N*-glycosylation site, using state-of-the-art NMR and mass spectrometry techniques. Even though all structures belong to the hybrid- or biantennary complex-type structures, the variety of epitopes is remarkable. In addition to the 3-*O*-sulfate present on the HNK-1-carrying structures, most of the glycans contain a 6-*O*-sulfated *N*-acetylglucosamine residue. This indicates the activity of a 6-*O*-sulfo-GlcNAc-transferase, which has not been described before in peripheral nervous tissue. The presence of the disialo-, galactosyl-, and 6-*O*-sulfosialyl-Lewis X epitopes provides evidence for glycosyltransferase activities not detected until now. The finding of such an epitope diversity triggers questions related to their function and whether events, previously attributed merely to the HNK-1 epitope, could be mediated by the structures described here.

The P0 glycoprotein consists of a single immunoglobulin-like domain in its extracellular part, a transmembranous domain, and a cytoplasmic tail. It is the most abundant protein constituent of peripheral myelin. P0 contains a single *N*-glycosylation site and heterogeneity in its glycosylation pattern that originates from variable contents of fucose, galactose, and sialic acid residues; sulfate; and the HNK-1 carbohydrate epitope (1–4). P0 appears at the initial stage of myelination and contributes to the formation and maintenance of myelin compaction as an adhesion molecule (5). The essential functional role of P0 in the processes of myelination has been demonstrated by creating P0 knockout mice, which show severe hypomyelination and myelin degeneration (5, 6). In humans, several neurological disorders such as Charcot-Marie-Tooth disease, Dejerine-Sottas disease, and congenital hypomyelination have been associated with mutations in the P0 gene (7).

It has been reported that the glycan moiety of P0 plays an important role in cell-cell adhesion via homophilic binding. This homophilic binding has been mapped to the SDNGT sequence composing amino acids 91–95, which harbors the single *N*-glycosylation site on P0 (8). Thus, it was observed that this glycopeptide fragment inhibits cell adhesion to a greater extent than the corresponding peptide without glycan (9). Non-glycosylated P0, produced by site-directed mutagenesis, does not show homophilic adhesion (10). In addition, amino acids 43–50 and 74–82 may also contribute to the homophilic binding in a non-carbohydrate-dependent manner (11). Occurrence of age-dependent alteration in the glycan moiety of P0 in the peripheral nerve (12) and mammalian spinal cord (5, 6, 13) has been reported, suggesting that the glycan heterogeneity might be regulated by alterations in physiological conditions, although details of the structural changes of the carbohydrate chain have not yet elucidated.

So far, attempts to identify the oligosaccharides on the P0 glycoprotein using mass spectrometry (2, 14) or various chromatographic techniques (3, 15, 16) have not provided conclusive data concerning the structures of these carbohydrates. Only recently have we described the detailed structural analysis of a major HNK-1-reactive oligosaccharide of the bovine peripheral myelin P0 glycoprotein (17).

In this study, a detailed structural analysis of the carbohydrates contained in the bovine P0 glycoprotein has been performed. The core structure of the carbohydrates and several epitopes, including HNK-1 (17) and 6-*O*-sulfosialyl-Lewis X (18), were identified using highly sensitive techniques for carbohydrate analysis such as high resolution magic angle spin-

* The costs of publication of this article were defrayed in part by the payment of page charges. This article must therefore be hereby marked "*advertisement*" in accordance with 18 U.S.C. Section 1734 solely to indicate this fact.

§ Both authors contributed equally to this work.

¶ Supported by European Commission DG-XII-E Postdoctoral Grant BIO4CT975071 (Biotechnology Program).

** Supported by Danish Technical Council Grant 9900687.

§§ To whom correspondence should be addressed: Bijvoet Center, Dept. of Bio-organic Chemistry, Utrecht University, P. O. Box 80075, NL-3508 TB Utrecht, The Netherlands. Tel.: 31-30-253-2184; Fax: 31-30-254-0980; E-mail: vlieg@pobox.uu.nl.

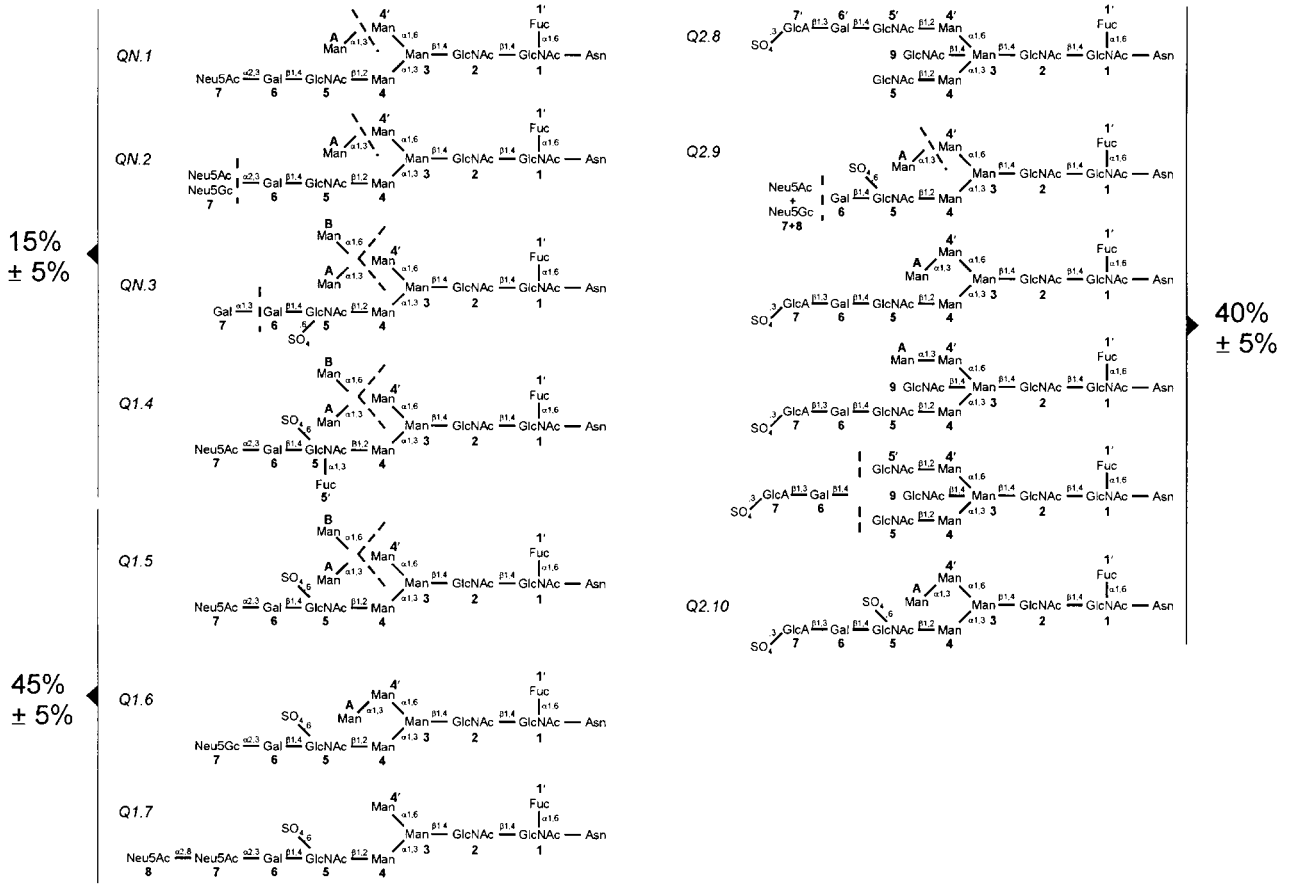

FIG. 1. **Structures of the bovine peripheral glycoprotein P0 glycans.** Structures are given with their corresponding fraction numbers and the numbering of the residues. *Dashed lines* indicate that the structures with and without the substituent were observed in the mass spectra. Percentages were derived from the high pH anion-exchange chromatography peak areas. *GlcA* is GlcUA.

ning (MAS)[1] ^{1}H NMR spectroscopy in a nano probe in combination with both MALDI-TOF and ESI mass spectrometry.

EXPERIMENTAL PROCEDURES

Isolation of P0 and Release and Isolation of the Carbohydrate Chains—The P0 isolation procedure and release of the carbohydrate chains were described previously by Voshol *et al*. (17). After removal of the protein and detergent, fractionation according to charge was performed on a Mono-Q column (1 ml; Amersham Pharmacia Biotech FPLC system) at a flow rate of 1 ml/min using the following NaCl gradient: 0–4 ml, 0 mM; 4–12 ml, 0–50 mM; and 12–20 ml, 50–500 mM; followed by a regeneration step at 1 M NaCl. The effluent was monitored at 214 nm. Further fractionation by high pH anion-exchange chromatography (19) was performed using a CarboPac PA-100 column (Dionex DX-500 system) with a 30-ml gradient from 100 to 600 mM sodium acetate in 0.1 M NaOH. Corresponding fractions from different runs were pooled, neutralized, and desalted on P2.

NMR Spectroscopy—Prior to NMR spectroscopic analyses in ^2H_2O, samples were exchanged twice in 99.9% ^2H_2O with intermediate lyophilization. For 5-mm probe and nano probe experiments, samples were finally dissolved in 500 and 40 μl of 99.96% ^2H_2O (MSD Isotopes), respectively. One- and two-dimensional ^{1}H NMR measurements in a 5-mm probe were carried out on a Bruker Daltonik AMX-500 or AMX-600 spectrometer (Bijvoet Center, Department of NMR Spectroscopy, Utrecht University). MAS ^{1}H NMR spectra were recorded on a Varian Unity Inova 500-MHz spectrometer equipped with a 4-mm observe ^{1}H NMR nano probe (Department of Chemistry, Carlsberg Laboratory). All spectra were measured at incoming temperatures of 300 K, which in the nano probe equals 302 K due to the fast spinning of the sample at ~2 kHz at the magic angle (54.7°). The one-dimensional spectra were acquired as one-pulse experiments with pre-saturation of the $^1HO^2H$ resonance. Acquisition data for the one-dimensional spectra were as follows: 2.0-s acquisition time, 2.0-s pre-saturation delay, and sweep width of 8000 Hz with the number of scans varying between 32 and 1024. One-dimensional experiments in a 5-mm probe were performed at a probe temperature of 285 K as described by Voshol *et al.* (17). ^{1}H chemical shifts (δ) were expressed by reference to internal acetone (δ 2.225) or acetate (δ 1.908). Two-dimensional spectra were recorded in a 5-mm probe with 400–600 t_1 experiments, and 96–163 free induction decays of 2048 data points were collected per t_1 experiment. In the nano probe, 468–1024 t_1 experiments and 32–128 free induction decays of 2048 complex data points were collected per t_1 experiment. Two-dimensional TOCSY spectra in the nano probe were acquired with a pre-saturation delay of 1.05–1.2 5. The mixing time was 80–90 ms using an adiabatic WURST 8 mixing waveform, with a total length of the adiabatic pulse of 0.4 ms and a sweep width of 20 kHz used with a 20-step supercycle (20). Two-dimensional TOCSY spectra in a 5-mm probe were recorded using a "clean" MLEV-17 spin-lock pulse (21–23) of 90–110 ms as described by Voshol *et al.* (17). A two-dimensional rotating frame NOESY spectrum in the nano probe was recorded with a mixing time of 200 ms. The mixing sequence was a continuous spin-lock pulse of a power level corresponding to a 90° pulse of 110-μs duration. Two-dimensional rotating frame NOESY spectra in a 5-mm probe (24) were recorded at spin-lock times of 150–225 ms as described by Voshol *et al.* (17). A two-dimensional NOESY spectrum (25) in a nano probe was acquired with a mixing time of 200 ms and pre-saturation delay of 1.2 s. A two-dimensional NOE spectrum in $^1H_2O/^2H_2O$ (9:1, v/v) using a 5-mm probe was obtained at pH 6.0 using phosphate buffer (50 mM Na_2HPO_4 and 50 mM NaH_2PO_4 containing 0.1 mM NaN_3) with offset at 10.01 ppm and a mixing time of 225 ms. Data sets were processed using locally developed software (J. A. van Kuik, Bijvoet Center, Utrecht University) as described by Voshol *et al.* (17).

Sialidase Treatment—Sialidase (*Clostridium perfringens*, Oxford Glycosciences) digestion was performed by incubating lyophilized ma-

[1] The abbreviations used are: MAS, magic angle spinning; MALDI-TOF, matrix-assisted laser desorption ionization time-of-flight; ESI, electrospray ionization; TOCSY, total correlation spectroscopy; NOE, nuclear Overhauser effect; NOESY, nuclear Overhauser effect spectroscopy; Neu5Ac, *N*-acetylneuraminic acid; Neu5Gc, *N*-glycolylneuraminic acid.

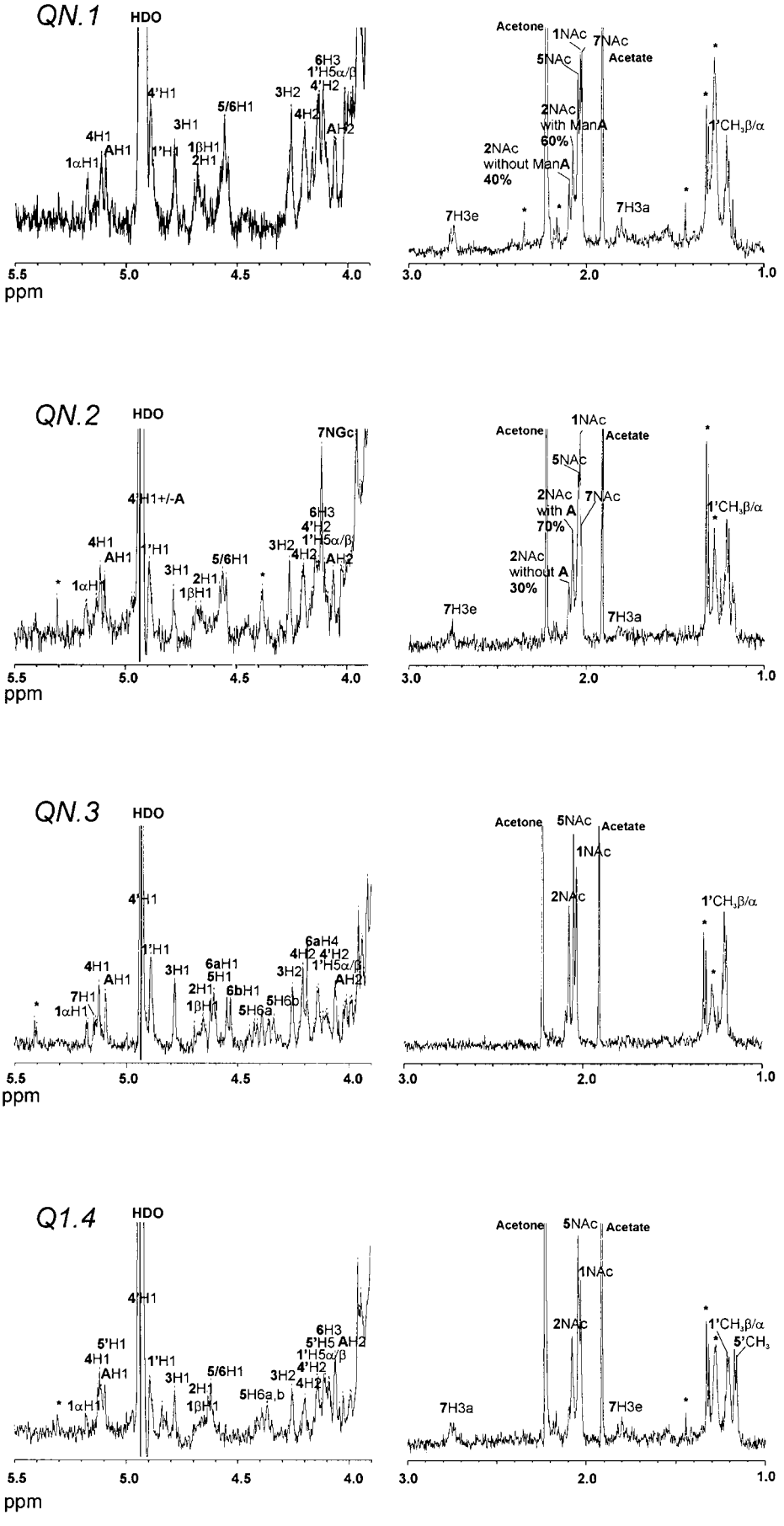

FIG. 2. **One-dimensional ^{1}H NMR spectra at 500 MHz of the bovine peripheral glycoprotein P0 glycans.** Spectra are given with their corresponding fraction numbers, and assignments correspond to the numbering of the residues, depicted in Fig. 1. QN.1–3, Q1.4–6, Q2.9, and Q2.10 are at 285 K (5-mm probe); Q1.7 is at 300 K (nano probe). In the spectrum of QN.3, the *6a* and *6b* notations correspond to Gal-6 with and without Gal-7, respectively. Peaks marked with *asterisks* did not originate from carbohydrate material as observed in the two-dimensional NMR spectra. The acetone and acetate peaks are set at 2.225 and 1.908 ppm, respectively. The HDO peak is at 4.92 ppm for 285 K and at 4.77 ppm at 300 K. *NAc*, *N*-acetyl; *NGc*, *N*-glycolyl.

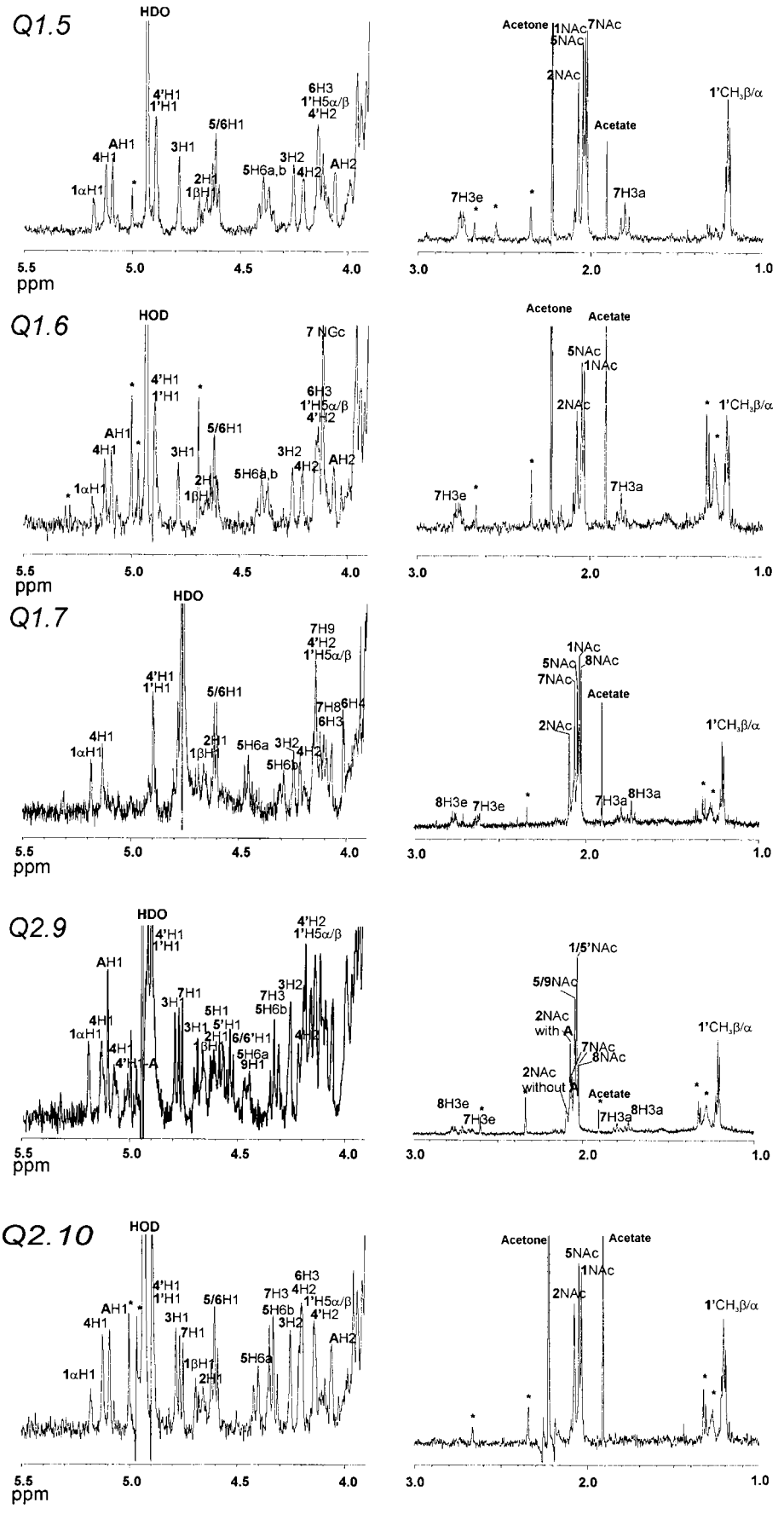

FIG. 2—*continued*

terial in 20 μl of 50 mM sodium acetate buffer (pH 5.0) with 20 milliunits of enzyme for 24 h at 37 °C. Subsequently, the reaction mixture was applied to a Millipore MC membrane filter (5000 nmwl (nominal molecular weight limit), 0.2 cm^2) and centrifuged at 15,000 rpm for 15 min. The effluent was lyophilized and permethylated as described below.

Permethylation—After sialidase digestion, the fractions QN.1 and

QN.2 were lyophilized and dried over diphosphorus pentoxide prior to permethylation. Permethylation was performed essentially as described by Ciucanu and Kerek (26). After quenching the reaction, the reaction mixture was washed three times with 700 μl of $CHCl_3$. The combined $CHCl_3$ fractions were washed three times with 1 ml of H_2O, dried under a stream of nitrogen, and dissolved in 10 μl of $CHCl_3$. For MALDI-TOF analysis, 0.5 μl was used.

Mass Spectrometry—Negative-ion mode ESI mass spectrometric analyses of fractions Q1.5 and Q2.10 were performed on an Esquire-LC™ quadrupole ion-trap spectrometer (Bruker Daltonik GmbH, Bremen, Germany). Samples were dissolved in 50 μl of deionized water/acetonitrile (1:1) and were introduced by infusion at a flow rate of 1 μl/min. Ions were scanned (scan range of 50–2100 Da) with a scan speed of 13,000 Da/s at unit resolution using resonance ejection at the hexapole resonance of one-third of the radio frequency (781,250 Hz). The calibration of the mass spectrometer was performed using ESI tuning mixture (Hewlett-Packard Co., Palo Alto, CA). Collision-induced dissociation (CID) tandem mass spectrometric experiments were performed using the quadrupole ion trap to select the precursor ion for fragmentation. Helium was used as collision gas, and the fragmentation energy applied on the end caps varied between 0.5 and 1.8 V. Recorded data were processed using Esquire-NT Version 3.1 software (Bruker Daltonik GmbH). Negative-ion mode mass spectrometric analyses of all other fractions were performed on a Reflex III MALDI-TOF spectrometer (Bruker Daltonik GmbH) equipped with a SCOUT ion source, a N_2 laser (337 nm), and a 2-GHz digitizer. The spectra were recorded over a mass range of 3000 Da in the reflectron mode using pulsed ion extraction and an acceleration voltage of 25 kV. Aliquots (0.5 μl) of fractions QN.1 and QN.2 (dissolved in $CHCl_3$ after desialylation and permethylation) were deposited on microcrystalline α-cyano-4-hydroxycinnamic acid surfaces and allowed to dry at ambient temperature. The α-cyano-4-hydroxycinnamic acid thin-layer preparation was performed as described by Vorm and Mann (27). The remaining fractions were dissolved in water, diluted 1:10 with trihydroxyacetophenone (17 g/liter) in 80% acetonitrile and 20% deionized water dosed with 1 mM diammonium citrate. Aliquots of ~0.5 μl were spotted on the target and allowed to dry at ambient temperature. External calibration was performed using a two-peptide mixture, which was measured using α-cyano-4-hydroxycinnamic acid as a matrix. Data recorded were processed using Bruker Daltonik XMASS/NT Version 5 software.

RESULTS

The carbohydrate pool released from P0 was fractionated into three fractions by anion-exchange chromatography on Mono-Q: QN (15 ± 5% of the total), Q1 (45 ± 5% of the total), and Q2 (40 ± 5% of the total), eluting at starting buffer without NaCl, starting buffer with a gradient of NaCl from 30 to 100 mM, and starting buffer with a gradient of NaCl from 100 to 400 mM, respectively. Since the Mono-Q pattern varied slightly from run to run, due to the remaining SDS in the mixture, we did not attempt to obtain a better resolution at this stage. Further fractionation by high pH anion-exchange chromatography (19) resulted in three main fractions for QN (QN.1–3), four main fractions for Q1 (Q1.4–7), and three main fractions for Q2 (Q2.8–10) (data not shown). Due to variations in the pulsed amperometric detection response, no estimation of the percentages for the individual fractions could be made. These combined fractions accounted for >90% of all glycans on P0. At this stage of purification, only three fractions were homogeneous according to one-dimensional ^{1}H NMR spectroscopy and mass spectrometry; nevertheless, no further purification was carried out in order to prevent any loss of material. Instead, the fractions were analyzed by a combination of mass spectrometry and state-of-the-art NMR spectroscopy. A description is given below of the characteristic features of each fraction, and the deduced structures are summarized in Fig. 1.

QN.1 and QN.2—The negative-ion mode MALDI-TOF mass spectra of QN.1 and QN.2 (data not shown) after sialidase treatment and permethylation showed two peaks at m/z 1985.0 and 2346.2 corresponding to permethylated Hex_4-dHex-$HexNAc_3$ $[M - H]^-$ and Hex_5-dHex-$HexNAc_3$ $[M - H]^-$, respectively, and several other pseudo-molecular ions corresponding to the same structures, but with different degrees of methylation. The one-dimensional ^{1}H NMR spectra of QN.1 and QN.2 (Fig. 2) revealed the structural reporter group signals (Table I) of a monosialylated hybrid-type structure as described previously (28). For QN.1, two methyl doublets were observed at δ 1.207 and 1.220 (Table I) belonging to the fucose residue α1,6-linked to the Asn-linked GlcNAc-1. The core fucosylation resulted in a downfield shift (~0.043 ppm) of the GlcNAc-2 H-1, which was linked to the GlcNAc-1 α-anomer. The two methyl doublets indicated the presence or absence of a Man-A residue, respectively (29). The observation of two GlcNAc-2 *N*-acetyl singlets at δ 2.096 and 2.078 (Fig. 2, QN.1) corroborated this finding. These structural features were also observed in most of the other heterogeneous fractions, confining the structures present in those fractions (Fig. 1) to the hybrid-type category. In the case of QN.2, the main constituent was a hybrid-type structure containing *N*-glycolylneuraminic acid, as evidenced by the presence of the *N*-glycolyl singlet at δ 4.116. In addition, the low intensity signal for *N*-acetyl at δ 2.028 (Fig. 2, QN.2) indicated that fraction QN.2 was contaminated with fraction QN.1. Also in this fraction, part of the structures carried the Man-A residue.

QN.3—The MALDI-TOF mass spectrum of QN.3 (Fig. 3) in the negative-ion mode revealed four pseudo-molecular ions at m/z 1500.7, 1662.7, 1824.7, and 1986.7 corresponding to Hex_4-dHex-$HexNAc_3(SO_3)$ $[M - H]^-$ and the Hex_5, Hex_6, and Hex_7 analogs, respectively. The structures containing Hex_4 and Hex_7 were the minor constituents of this fraction, and the latter structure indicated the existence of a terminal Hex-Hex sequence. The one-dimensional ^{1}H NMR spectrum of QN.3 (Fig. 2) showed the reporter group signals of an asialo hybrid-type structure (30), and the observed chemical shifts are summarized in Table I. The observation of the downfield shift of the GlcNAc-5 H-6a and H-6b resonances to δ 4.405 and 4.348 (Fig. 2, QN.3) revealed the sulfation of this residue as observed by De Waard *et al.* (31). Two additional α-anomeric signals were observed with respect to QN.1 in the NMR spectrum recorded at 300 K (data not shown) at δ 4.912 and 5.146. The resonance at δ 4.912 corresponded to H-1 of Man-B (28), and the signal at δ 5.146 originated from H-1 of the Hex(α1-)Gal structure (32, 33). In the TOCSY spectrum (Fig. 4, QN.3), the α-anomeric spin system at δ 5.146 displayed a typical set of three cross-peaks of a Gal residue (Gal-7). Two anomeric resonances were observed for Gal-6 at δ 4.600 and 4.542. The set of cross-peaks on the anomeric track at δ 4.600 revealed the substitution at OH-3 of this Gal-6 with Gal-7 (32). However, the three cross-peaks observed on the anomeric track of Gal-6 at δ 4.542 clearly indicated that this residue was not substituted (32). In summary, fraction QN.3 consists of four hybrid-type structures differing in mass. The Hex_4- and Hex_7-containing structures represented a single compound, whereas the other two could each be present in different glycoforms (Fig. 1).

Q1.4—The MALDI-TOF mass spectrum of Q1.4 (Fig. 3) yielded mainly one peak in the high mass region at m/z 2099.7 corresponding to the $[M - H]^-$ pseudo-molecular ion of Neu5Ac-Hex_5-$dHex_2$-$HexNAc_3(SO_3)$. In addition, the sodiated ($[M + Na - 2H]^-$, m/z 2121.7) and potasiated ($[M + K - 2H]^-$, m/z 2137.7) pseudo-molecular ions were observed, as well as low intensity signals at m/z 2283.8 ($[M + Na - 2H]^-$) and 1959.7 ($[M + Na - 2H]^-$), which corresponded to the structures containing one Hex residue more or less, respectively. The peaks observed below m/z 1959.7 were identified as metastable ions based on the characteristic isotope patterns. The NMR data derived from one-dimensional ^{1}H NMR and two-dimensional TOCSY and NOESY experiments, as summarized in Table I, showed two major differences when compared with those of QN.1. In the one-dimensional spectrum (Fig. 2, Q1.4),

TABLE I

^{1}H NMR parameters of the P0 glycoprotein oligosaccharides

Shown are the chemical shifts (in ppm, referenced to internal acetone (δ 2.225) or internal acetate (δ 1.908)) of the structural reporter groups derived from one- and two-dimensional NMR measurements at 285 K, unless marked with an asterisk. Values marked with an asterisk correspond to one-dimensional NMR and two-dimensional measurements at 300 K. For reference, the structures and the numbering of the residues are given in Fig. 1.

Reporter group	Residue	QN.1[a]	QN.2	QN.3[b]	Q1.4	Q1.5	Q1.6	Q1.7	Q2.8	Q2.9[c]	Q2.10
H-1	GlcNAc-1α/β	5.175/4.695	5.175/4.691	5.178/4.697	5.178/4.962*	5.180/4.683*	5.182/4.683*	5.182*/4.689*	5.178*/n.d.	5.180/4.689	5.179/4.692
	GlcNAc-2α/β	4.651/4.666*	4.653*/4.660*	4.657/4.665	4.654*/4.657*	4.653/4.657	4.650*/n.d.	4.653*/n.d.	4.651/4.659	4.660/n.d.	4.658/n.d.
	Man-3	4.784	4.784	4.784	4.782	4.784	4.782	4.779*	4.685	4.785/4.689	4.783
	Man-4	5.115	5.114	5.124	5.116	5.125	5.124	5.130*	5.059	5.123/5.060	5.125
	Man-4′	4.894*	4.893*	4.892	4.895*	4.901	4.892	4.895*	5.003	4.894/5.000	4.895
	Man-A	5.095	5.095	5.095	5.095	5.095	5.094			5.093	5.093
	Man-B			4.912							
	GlcNAc-5	4.573	4.567	4.616	4.621	4.610	4.608	4.605*	4.565	4.614/4.606	4.576
	GlcNAc-5′								4.570	4.570	
	Gal-6	4.548	4.552	4.542/4.600*	4.615	4.624	4.625	4.605*	4.534	4.524/4.555	4.597
	Gal-6′								4.534	4.529	
	Gal-7			5.146							
	GlcUA-7								4.760	4.758	4.758
	GlcNAc-9								4.456	4.456	
	Fuc-1′ α/β	4.890*/4.904*	4.890*/4.902*	4.895*/4.899*	4.894*/4.910*	4.901/4.898*	4.892/4.896*	4.889*/4.900*	4.899/4.909	4.882*/4.889*	4.895/HOD
	Fuc-5′				5.112						
H-2	GlcNAc-1			3.89*	3.89*	3.89	3.89*	3.88	3.89	3.89	3.89*
	GlcNAc-2			3.77*	3.772*	3.78	3.77*	3.77	3.74	3.75	3.74*
	Man-3	4.257	4.260	4.256	4.256	4.254	4.254	4.241*	4.173	4.254/4.110	4.253
	Man-4	4.196	4.195	4.208	4.197	4.212	4.206	4.210*	4.252	4.210/4.258	4.210
	Man-4′	4.131	4.136	4.138	4.140	4.144	4.135	4.139*	4.159	4.140/4.157	4.141
	Man-Λ	4.063	4.061	4.064	4.060	4.061	4.062			4.059	4.060
	GlcNAc-5			3.77*	3.77*	3.77	3.78*	3.76	3.49	3.74	3.78*
	Gal-6			3.52*/3.64*	3.50*	3.55	3.56*	3.55	3.68	3.69	3.76*
	Gal-6′								3.69	3.69	
	Gal-7			3.86*							
	GlcUA-7								3.59	3.59	3.580
	Fuc-1′			3.79*	3.80*	3.75	3.79*	3.78		3.78	
	Fuc-5′				3.67*						
H-3	GlcNAc-2			3.77*	3.77*	3.78	3.77*	3.77	3.82	3.75	3.77*
	Man-3			3.78*	3.78*	3.78	3.78*	3.77	3.87	3.78	3.78*
	Man-4			3.90*	3.89*	3.90	3.90*	3.90	3.92		3.89*
	Man-4′			3.95	3.95	3.95	3.97*	3.95	3.83	3.95	3.95*
	Man-A			3.89*	3.89*	3.89	3.89*			3.88	3.88*
	GlcNAc-5			3.77*	3.77*	3.72	3.74*	3.76		3.61	3.73*
	Gal-6	4.114	4.100	3.66*	4.11	4.13	4.13*	4.11	4.198	4.190/4.110	4.201
	Gal-6′								4.190	4.185	
	GlcUA-7								4.328	4.327	4.332
	Neu5Ac/Gc-7e	2.755	2.752		2.748	2.748	2.768	2.630*		2.750/2.652	
	Neu5Ac/Gc-7	1.803	1.803		1.797	1.806	1.820	1.777*		1.794	
	Neu5Ac-8e/a							2.760*/1.738*		2.750/1.736	
	Fuc-1′			3.89*	3.90*	3.91	3.90*	3.90		3.91	
H-4	GlcNAc-Ac-2			3.77*	3.77*	3.73	3.75*	3.77		3.75	3.77*
	Man-3					3.66	3.64*		4.10	3.65	3.65*
	Man-4			3.51*	3.51*	3.50	3.51*		3.46		3.50*
	Man-4′					3.75	3.75*	3.73	3.46	3.73	3.74*
	Man-A			3.67*	3.67*	3.67	3.66*			3.67	3.67*
	GlcNAc-5			3.65*	4.03*					3.48	
	Gal-6			3.93*/4.17*	3.95*	3.97	3.97*	4.00	3.83	3.82	3.83*
	Gal-6′								3.83	3.82	
	GlcUA-7								3.71	3.70	3.70*
	Neu5Ac/Gc-7				3.67*	3.68	3.80*	3.60			
H-5	GlcNAc-2			3.59*	3.59*	3.59	3.59*	3.58	3.57	3.58	3.58*
	Man-3								3.53		
	Man-4					3.74	3.76*				
	Man-4′								3.62		
	Man-A			3.78*	3.78*	3.76	3.76*			3.77	3.76*
	GlcNAc-5			3.80*	3.79*	3.80	3.80*	3.82			3.80*
	Neu5Ac/Gc-7				3.83*	3.87	3.94*	3.80			
	GlcUA-7								3.79	3.80	3.80*
	Fuc-1′α/β	4.114/4.131	4.106/4.140	4.11/4.14	4.09/4.14	4.10/4.14	4.11/4.13	4.10*/4.14*	4.11/4.14	4.10/4.14	4.10*/4.14*
	Fuc-5′				4.834						
H-6	GlcNAc-5α/β			4.405/4.348	4.401/4.356	4.405/4.355	4.396/4.367	4.450*/4.295*			4.413/4.340
	Neu5Ac/Gc-7					3.63	3.75*				
H-8	Neu5Ac-7							4.117*			
H-9a	Neu5Ac-7							4.139*			
NGc[d]	Neu5Gc-7		4.116				4.113			4.110	
NAc	GlcNAc-1	2.037	2.037	2.037	2.038	2.037	2.037	2.038*	2.038	2.037	2.036
	GlcNAc-2	2.096/2.078	2.098/2.078	2.078	2.077	2.078	2.077	2.095*	2.098	2.077/2.096	2.077
	GlcNAc-5	2.049	2.046	2.053	2.042	2.050	2.050	2.049*	2.066	2.051	2.051
	GlcNAc-5′								2.038	2.037/2.066	
	Neu5Ac-7	2.028	2.028		2.026	2.028		2.064*		2.025/2.066	
	Neu5Ac-8							2.028*		2.025	
	GlcNAc-9								2.053	2.051	
CH_3	Fuc-1′α/β	1.207/1.220	1.207/1.220	1.207/1.219	1.202/1.213	1.207/1.218	1.207/1.218	1.209*/1.219*	1.208/1.220	1.207/1.218	1.207/1.218
	Fuc-5′				1.166						

[a] Double values for the *N*-acetyl of GlcNAc-2 due to the absence and presence of Man-A.

[b] Double values for Gal-6 due to the absence and presence of Gal-7.

[c] Multiple values due to the presence of several structures in the fraction (see Fig. 1).

[d] NGc, *N*-glycolyl; NAc, *N*-acetyl.

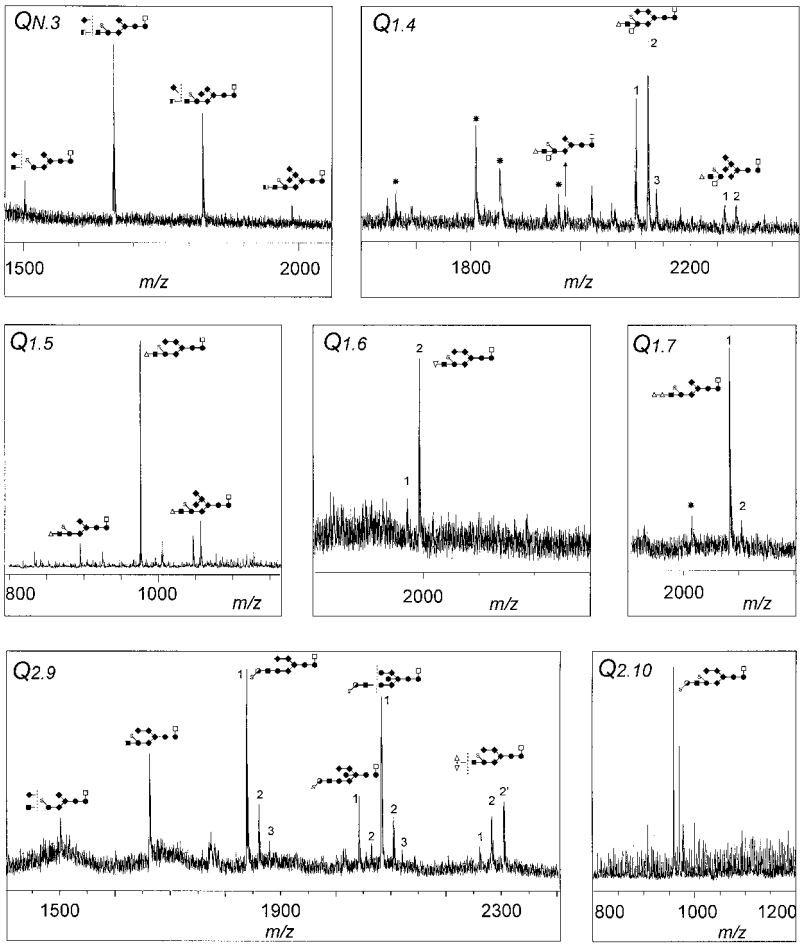

FIG. 3. **MALDI-TOF (QN.3, Q1.4, Q1.6, Q1.7 and Q2.9) and ESI (Q1.5 and Q2.10) mass spectra of the underivatized bovine peripheral glycoprotein P0 glycans.** Peaks marked with *asterisks* stem from *meta*-stable ions. *Peak 1*, $[M - H]^-$; *peak 2*, $[M + Na - 2H]^-$; *peak 2′*, $[M + 2Na - 3H]^-$; *peak 3*, $[M + K - 2H]^-$. □, Fuc; ●, GlcNAc; ♦, Man; ■, β-Gal; △, Neu5Ac; ▽, Neu5Gc; ◑, GlcUA; *S*, OSO_3; ◧, α-Gal.

the α-anomeric proton at δ 5.112 in combination with the CH_3 doublet at δ 1.166 evidenced the presence of α1,3-fucosylation of GlcNAc-5 (34). Moreover, the observation of the downfield-shifted resonances of the GlcNAc-5 H-6a and H-6b atoms, as in QN.3, demonstrated the 6-*O*-sulfation of this residue (31). The combined data pointed toward the presence of a 6-*O*-sulfosialyl-Lewis X structure in this fraction (Fig. 2). The downfield shift of H-3 on the TOCSY track of Gal-6 H-1 (Fig. 4, Q1.4) indicated that Neu5Ac-7 was α2,3-linked to Gal-6. The two-dimensional NOESY NMR spectrum (data not shown) recorded using nano probe MAS NMR spectroscopy, showed NOEs, between Fuc-5′ H-1 and Gal-6 H-1 and between Gal-6 H-1 and GlcNAc-5 H-2/3/4, providing evidence for the existence of this structure.

Q1.5 and Q1.6—The negative-ion mode ESI mass spectrum of fraction Q1.5 (Fig. 3) showed one high intensity peak at *m/z* 976.2 ($[M - 2H]^{2-}$) and two low intensity peaks at *m/z* 895.2 and 1057.2 ($[M - 2H]^{2-}$). After spectral deconvolution, the pseudo-molecular masses corresponded to Neu5Ac-Hex_5-dHex-$HexNAc_3(SO_3)$ and the Hex_4 and Hex_6 analogs, respectively. CID mass spectrometric analysis (data not shown) of *m/z* 976.2 yielded several fragments ions. The most important ions could be assigned to $[M - dHex\text{-}HexNAc]^-$ (*m/z* 801.56) and $[M - Neu5Ac\text{-}Hex_2(SO_3)\text{-}HexNAc\text{-}CH_6O_3]^-$ (*m/z* 977.12). The negative-ion mode MALDI-TOF spectrum of fraction Q1.6 (Fig. 3) revealed only one intense peak at *m/z* 1991.68 corresponding to the $[M + Na - 2H]^-$ pseudo-molecular ion of Neu5Gc-Hex_5-dHex-$HexNAc_3(SO_3)$. The one-dimensional ^1H NMR spectrum of fraction Q1.5 (Fig. 2) was similar to that of QN.1, and the chemical shifts are summarized in Table I. The main difference was the downfield shift of the GlcNAc-5 H-6a and H-6b resonances as observed for fractions Q1.3 and Q1.4, indicating 6-*O*-sulfation at this residue (31). The sulfation of GlcNAc-5 induced a 0.07-ppm downfield shift of Gal-6 H-1. The absence of fucosylation at GlcNAc-5, when compared with fraction Q1.4, resulted in a 0.01-ppm upfield shift of the GlcNAc-5 H-1 resonance and the slightly downfield shift of the GlcNAc-5 *N*-acetyl signal of this residue. The one-dimensional ^1H NMR spectrum of fraction Q1.6 (Fig. 2) was similar to that of Q1.5, and the chemical shifts are summarized in Table I. The peak at δ 4.113 and the absence of the *N*-acetyl resonance at δ 2.028 in the one-dimensional NMR spectrum of Q1.6, when compared with that of Q1.5, demonstrated that in Q1.6, Neu5Gc was present instead of Neu5Ac.

Q1.7—The negative-ion mode MALDI-TOF mass spectrum of Q1.7 (Fig. 3) showed two pseudo-molecular ions at *m/z* 2082.81 and 2104.77 ($[M - H]^-$ and $[M + Na - 2H]^-$, respectively) belonging to Neu5Ac_2-Hex_4-dHex-$HexNAc_3(SO_3)$. The one-dimensional ^1H NMR spectrum of this structure (Fig. 2) showed reporter group signals as observed for fraction Q1.5 (Table I) with the following differences. An additional *N*-acetyl signal at δ 2.064 and additional H-3e (δ 2.630) and H-3a (δ 1.738) peaks revealed the presence of two Neu5Ac residues, supporting the mass spectrometric observation and demonstrating the presence of the Neu5Ac(α2–8)Neu5Ac(α2–3)Gal structure (35). The presence of signals at δ 4.117 and 4.139 stemming from Neu5Ac-7 H-8 and H-9, respectively, as observed previously for Neu5Ac(α2–8)Neu5Ac(α2-)-containing structures (36), confirmed the aforementioned structure. Since no H-3e signal was observed at δ 1.666 (37), the presence of a Neu5Ac(α2–8)Neu5Ac(α2–6)Gal structure could be excluded.

Q2.8—Fraction Q2.8 was described extensively by Voshol *et al.* (17). Interestingly, this fraction contained only one structure, which carried the HNK-1 epitope at the Man-4′ branch, as evidenced by the NMR data (Table I).

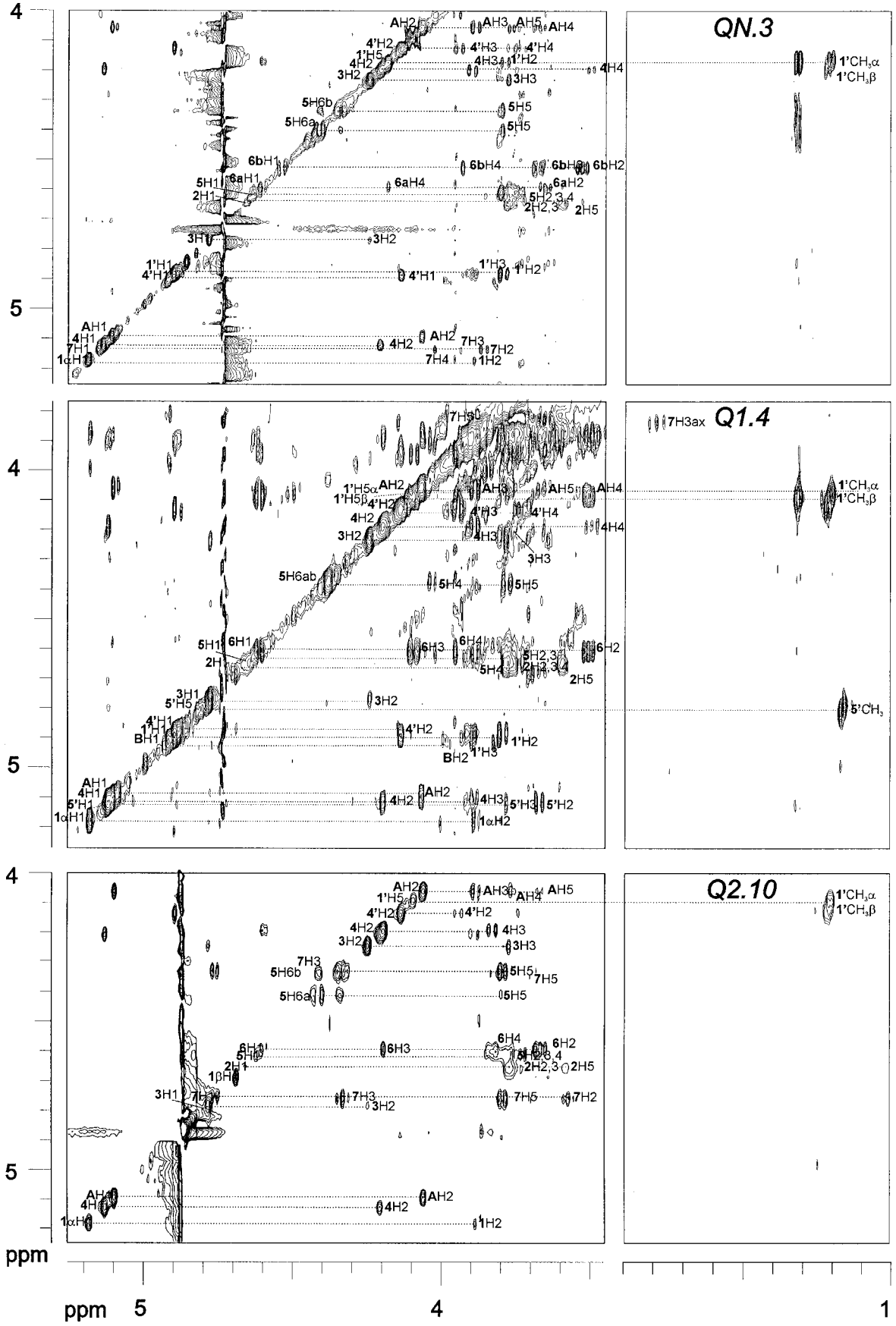

FIG. 4. **Two-dimensional ^{1}H TOCSY spectra of the carbohydrate structures of QN.3, Q1.4, and Q2.10.** Parts of TOCSY spectra recorded at 500 MHz are shown. The spectra of QN.3 and Q1.4 were recorded at 300 K with the MAS NMR nano probe. The spectrum of Q2.10 was recorded at 285 K with the normal probe. For comparison, the structures and the numbering of residues are given in Fig. 1. In the spectrum of QN.3, the *6a* and *6b* notations correspond to Gal-6 with and without Gal-7, respectively.

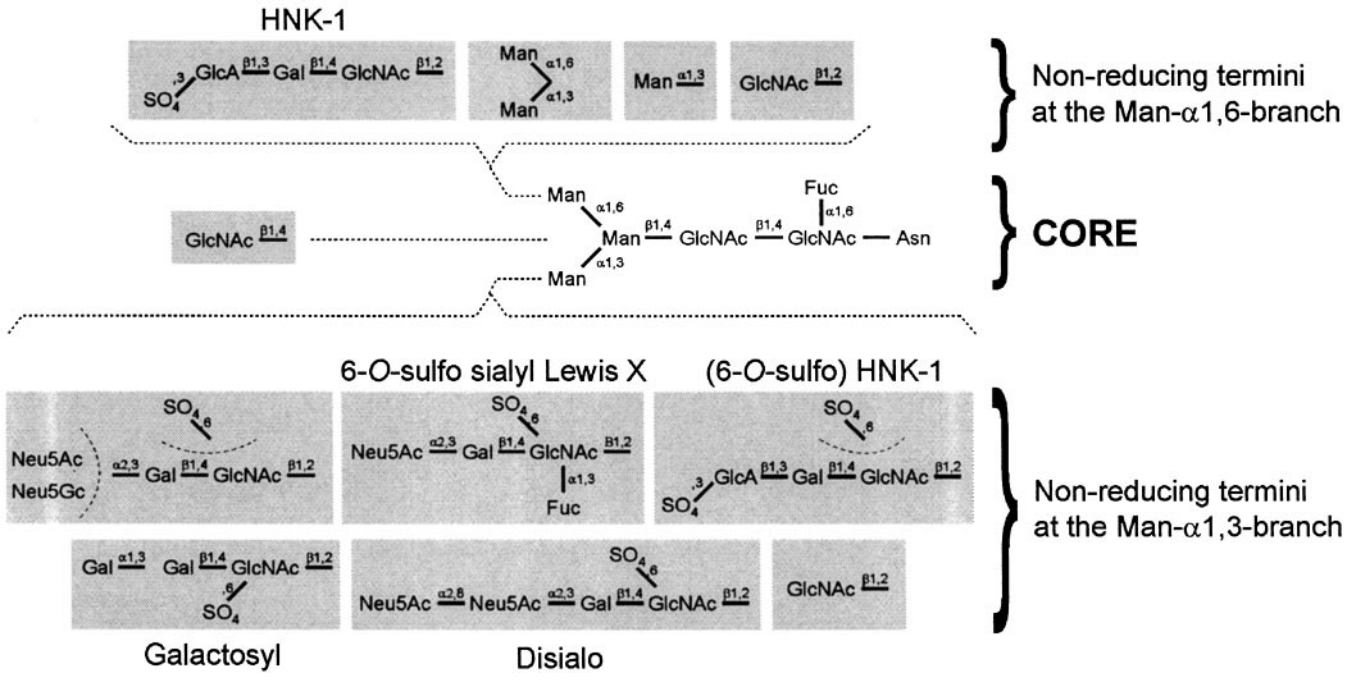

FIG. 5. **Summary of the structures of the PO glycans, divided into core region, and non-reducing termini of the Man-α 1,6- and Man-α 1,3-branches.**

Q2.9—The negative-ion mode MALDI-TOF spectrum of Q2.9 (Fig. 3) revealed the presence of a heterogeneous mixture by the observation of peaks at *m/z* 1500.00, 1662.84, 1838.73, 2041.80, 2082.78, and 2260.79. The assignments of the peaks to $[M - H]^-$ pseudo-molecular ions was corroborated by the observation of their $[M + Na - 2H]^-$ analogs. The peak at *m/z* 2260.79 corresponded to Neu5Gc-Neu5Ac-Hex_5-dHex-$HexNAc_3(SO_3)$. The two peaks at *m/z* 1500.0 and 1662.84 corresponded to Hex_4-dHex-$HexNAc_3(SO_3)$ and Hex_5-dHex-$HexNAc_3(SO_3)$, respectively, similar to the structures found in fraction QN.3 (Fig. 2), and originated from degradation of Neu5Gc-Neu5Ac-Hex_5-dHex-$HexNAc_3(SO_3)$ upon storage. The presence of Neu5Ac in Q2.9 was corroborated in the one-dimensional ^{1}H NMR spectrum (Fig. 2) by the observation of the low intensity multiplets originating from the H-3a and H-3e signals. The presence of Neu5Gc was evidenced by the characteristic *N*-glycolyl resonance at δ 4.11. This signal coincided with H-3 of Gal-6. The anomeric region of the one-dimensional ^{1}H NMR spectrum (Fig. 2, Q2.9) showed the presence of the Man-4 and Man-4′ signals as observed in fraction Q2.8 (Table I), indicating a chain elongation at the Man-4′ branch. In addition the Man-A and Man-4 signals were observed, revealing a chain elongation at the Man-4 branch. The presence of a bisecting GlcNAc-9 in some of the structures was evidenced by the anomeric signal at δ 4.456 and by the two Man-3 H-1 signals (Table I and Fig. 2, Q2.9) (17). Also, the signals were observed originating from 3-*O*-SO_3H-GlcUA-7 H-1 and H-3 and from 6-*O*-SO_3H-GlcNAc-5 H-6a and H-6b, as in fraction Q2.8 (Table I). The high field region of the one-dimensional ^{1}H NMR spectrum showed at least five *N*-acetyl signals (Table I) with different intensities. Furthermore, the methyl doublet from the core fucose was appreciated. The GlcNAc-2 *N*-acetyl signals at δ 2.077 and 2.096 (in a ratio of 5:1) revealed that ~20% of the structures had the chain elongation at the Man-4′ branch. The peak at *m/z* at 2028.78 in the mass spectrum was identified as the structure present in fraction Q2.8 and possibly its isomer bearing the HNK-1 epitope at the Man-4 branch (Fig. 2). The peak at *m/z* 2041.78 was then assigned to the structure containing the bisecting GlcNAc-9 and Man-A, instead of GlcNAc-5′ (Fig. 2), and the peak at *m/z* 1838.73 was assigned to the same structure without the bisecting GlcNAc-9 (Fig. 2).

Q2.10—The negative-ion mode ESI mass spectrum of Q2.10 (Fig. 3) revealed only one peak at *m/z* 958.6 ($[M - 2H]^{2-}$; $[M - H]^-$, *m/z* 1918.21). Mass spectra recorded after collision-induced dissociation (data not shown) of this peak yielded several fragments suitable for assigning the structure. The ion at *m/z* 1662.28 corresponded to $[M - HexUA(SO_3)]^-$, and the ion at *m/z* 1500.23 could be attributed to $[M - HexUA(SO_3)\text{-}Hex]^-$. The structure was identified as HexUA-Hex_5-dHex-$HexNAc_3(SO_3)_2$. In the one-dimensional ^{1}H NMR spectrum (Fig. 2, Q2.10), the anomeric region revealed signals, which were also observed for fraction Q1.6 (Table I) and, in addition, the presence of the signals of GlcUA-7 H-1 and H-3 and the downfield-shifted Gal-6 H-3 signal (Table I). The downfield-shifted GlcNAc-5 H-6a and H-6b resonances proved the C-6 sulfation of this residue (31). The *N*-acetyl region showed three signals, which originated from the GlcNAc residues, since no Neu5Ac was present. In the two-dimensional TOCSY spectrum (Fig. 4, Q2.10), the anomeric tracks of GlcNAc-1, -2, and -5 and those of Man-3, -4, and -A were identical to those observed for fraction Q1.6 (data not shown), allowing the identification of the structure (Fig. 2). The anomeric tracks of 3-*O*-SO_3H-GlcUA-7 and Gal-6 were identical to those observed for Q2.8, thus proving the position of the second sulfate group (17). This demonstrated that the HNK-1 epitope containing a sulfate group on GlcNAc C-6 was situated on Man-4 in fraction Q2.10.

DISCUSSION

In this study, we describe the detailed structural characterization of the *N*-linked glycans present on bovine peripheral myelin P0 using state-of-the-art NMR and mass spectrometry techniques. These glycans occur in addition to the core-fucosylated biantennary structure carrying a bisecting GlcNAc and the HNK-1 epitope on the Man-4′ branch that was characterized previously by us (17).

The isolation of myelin P0 proved to be extremely laborious; and therefore, only a limited amount of pure P0 could be obtained. Fractionation of the carbohydrate pool, after being released from the protein backbone, had to be limited as much as possible in order to prevent the loss of precious material. As

a result, most of the 10 fractions contained several structurally related glycoforms and had to be analyzed as mixtures. To perform the structural analysis successfully, ultrasensitive analytical methods capable of providing detailed structural information on such complex samples had to be employed. The newly developed nano probe MAS ^{1}H NMR technique allows the structural analysis of nanomolar quantities of material in solution. So far, this technique has scarcely been applied in structural carbohydrate analysis (38–40). The nano tube, which holds a volume of 40 μl, is normally spun at ~2 kHz at the magic angle (54.7°). Spinning at the magic angle removes magnetic susceptibility-induced line broadening and/or contributions from homonuclear dipolar couplings. With the novel probes and the use of gradients, it is possible to apply existing solution state NMR techniques for solving challenging structural problems. In the case of the P0 glycoprotein, the MAS ^{1}H NMR technique was complemented by sensitive mass spectrometric analyses.

The structures identified were for 75 ± 5% of the hybrid-type and for 25 ± 5% of the biantennary complex-type, carrying a distinct variety of structures at the Man-4 branch. All structures were core-fucosylated. Interestingly, Burger *et al.* (1), who studied P0 from human sciatic nerve by Western blot analysis and affinity chromatography, observed predominantly tri- and tetraantennary oligosaccharides (~80%), in addition to biantennary (10%) and oligomannose and/or hybrid (10%) oligosaccharides. This result may point to species-specific structures. In a study on human material, Field *et al.* (3) used enzymatic or chemical degradation in conjunction with chromatographic techniques for identification. They described the presence of HNK-1-positive carbohydrates, probably hybrid-type structures, containing either one sulfate residue (80%) or three sulfate residues (20%) in combination with sialylation.

Among the different structures we observed, the HNK-1 epitope (3-*O*-SO_3H-GlcUA(β1–3)Gal(β1–4)GlcNAc), detected in fractions Q2.8–10, has been well documented. This major carbohydrate epitope is prominently present in the nervous system and is carried by a variety of cell-surface glycolipids as well as glycoproteins (41). The antigen has been found to be one of the factors responsible for the precise cell adhesion and recognition processes that underlie the interaction of neural cells (42). It has also been implicated in interactions with laminin and peripheral nerve regeneration (43, 72–77). This carbohydrate antigen, also found in the retina and on HNK cells, is the main target of IgM molecules from patients with peripheral demyelination neuropathies (44, 78). Especially the sulfate ester within the epitope seems to play an essential role in the myelin assembly during development (45) and outgrowth of neurites (46). The sulfation of glucuronic acid, which occurs at the onset of myelination and regeneration and ceases after development, is mediated by a highly specific HNK-1 sulfotransferase (47, 48). In this context, the presence of the 6-*O*-sulfo-GlcNAc oligosaccharides (fractions Q1.4–2.10) and specifically the 6-*O*-sulfo-HNK-1 epitope, observed in fraction Q2.10 is interesting since it implies another sulfotransferase activity. Of the various 6-*O*-sulfo-GlcNAc-transferases identified thus far (49–52, 79), only one report describes the existence of a nervous system-involved sulfotransferase (53), which showed a high degree of homology to a family of 6-*O*-sulfotransferases, some of which are expressed also in brain (50, 54, 80, 81).

The observation of the 6-*O*-sulfosialyl-Lewis X and non-fucosylated precursors as capping epitopes was surprising. The terminal Neu5Ac/Gc(α2–3)Gal(β1–4)[6-*O*-SO_3H]GlcNAc structure is very uncommon and has been found only in *N*-glycans of the glycoprotein family (ZP3) from zona pellucida (55). The 6-*O*-sulfosialyl-Lewis X epitope has been identified as a potent inhibitor of the leukocyte adhesion molecule L-selectin (18), and its structure, function, and biosynthesis have been described by Kimura *et al.* (56). It is intriguing that we found its presence on the very same molecule that carries the HNK-1 antigen that also binds to L-selectin (57, 58). Previously, it has been suggested that the sulfoglucuronylparagloboside (containing the HNK-1 epitope) acts as the ligand for L-selectin in inflammatory disorders of both the central and peripheral nervous systems to regulate the invasion of activated lymphocytes into the brain (58). It is suggested that the expression of the 6-*O*-sulfosialyl-Lewis X structure serves the same purpose.

The α-galactosyl epitope (59) in combination with a 6-*O*-sulfated GlcNAc (Gal(α1–3)Gal(β1–4)6-*O*-SO_3H-GlcNAc), as observed in fraction QN.3, has not been described before in glycoproteins. The non-sulfated analog has been found on the *N*-linked glycans of mouse oocyte ZP3 (60), porcine thyroglobulin (31), and IgG1 antibodies produced by murine and transfectoma cell subclones (61) and has also been observed on gangliosides (33). The Gal(α1–3) linkage to the reducing terminal GalNAc in *O*-linked glycans was found to be present in significant quantities only in brain (62) and nervous tissue glycoproteins (63). Whether the presence of this α-galactosyl epitope, which has been identified as the major xenoantigen in pig-to-man transplants, is due only to the availability of the appropriate enzyme and donor substrate or whether it is functionally significant remains to be clarified. In fraction Q1.7 a second terminal structure was observed (Neu5Ac(α2–8)Neu5Ac(α2–3)Gal(β1–4)6-*O*-SO_3H-GlcNAc), which is completely new in *N*-linked glycans from glycoproteins. The disialo terminal epitope has been observed on glycosphingolipids from bovine brain (35) and frog brain (64) and in a variety of glycoproteins (65, 82–88), although never in combination with a sulfated GlcNAc. This structure, when present in higher polymeric forms as the so-called unusual polysialic acid associated with the neural cell adhesion molecule (N-CAM), is known to function in cell adhesion, differentiation, signal transduction, and surface expression of stage-specific developmental antigens. It indicates the expression of a sialyltransferase capable of generating the α2,8 linkage (66). Recently, Sato *et al.* (67) demonstrated the presence of this non-sulfated structure on many mammalian brain glycoproteins, using specific antibodies. It is more prominent in adult than in embryonic porcine brain tissue, suggesting a developmental regulation.

In summary, the nano probe MAS ^{1}H NMR spectroscopic and mass spectrometric techniques employed in this study, being at least a factor of 5 more sensitive than traditional methods, have demonstrated to be very powerful tools for the characterization of the *N*-glycans on the P0 glycoprotein from bovine peripheral myelin. The identification of the epitope library may bring us one step closer to the understanding of the relationship between the carbohydrates present and their putative functions in neural tissue (68–71). The observation of predominantly hybrid- and biantennary complex-type structures is remarkable. It is, however, very likely that the already mentioned spatiotemporally regulated and species-dependent expression causes the variety of epitopes observed. Although the glycosylation machinery is apparently fully operational, no higher antennary structures have been observed in bovine material, which might point toward a very subtle modulation of the glycan heterogeneity by the down-regulation of specific glycosyltransferases. The functional significance of the observed structural diversity poses a new challenging question.

Acknowledgments—We thank Drs. Y. E. M. van der Burgt, A. Schneider, and F. J. Mayer-Posner (Bruker Daltonik GmbH) for allowing the use of the Reflex III and Esquire-LC mass spectrometers and

help with the measurements. We acknowledge Dr. B. O. Petersen for help with the interpretation of the nano probe NMR data.

REFERENCES

1. Burger, D., Simon, M., Perruisseau, G., and Steck, A. J. (1990) *J. Neurochem.* **54,** 1569–1575
2. Uyemura, K., and Kitamura, K. (1991) *Comp. Biochem. Physiol. C Comp. Pharmacol.* **98,** 63–72
3. Field, M. C., Wing, D. R., Dwek, R. A., Rademacher, T. W., Schmitz, B., Bollensen, E., and Schachner, M. (1992) *J. Neurochem.* **58,** 993–1000
4. Badache, A., Burger, D., Villarroya, H., Robert, Y., Kuchler, S., Steck, A. J., and Zanetta, J.-P. (1992) *Dev. Neurosci.* **14,** 342–350
5. Giese, K. P., Martini, R., Lemke, G., Soriano, P., and Schachner, M. (1992) *Cell* **71,** 565–576
6. Martini, R., Zielasek, J., Toyka, K. V., Giese, K. P., and Schachner, M. (1995) *Nat. Genet.* **11,** 281–286
7. Warner, L. E., Hilz, M. J., Appel, S. H., Killian, J. M., Kolodny, E. H., Karpati, G., Carpenter, S., Watters, G. V., Wheeler, C., Witt, D., Bodell, A., Nellis, E., Van Broeckhoven, C., and Lupski, J. R. (1996) *Neuron* **17,** 451–460
8. Yoshida, M., and Colman D. R. (1996) *Neuron* **16,** 1115–1116
9. Yazaki, T., Miura, M., Asou, H., Kitamura, K., Toya, S., and Uyemura, K. (1992) *FEBS Lett.* **307,** 361–366
10. Filbin, M. T., and Tennekoon, G. I. (1993) *Cell Biol.* **122,** 451–459
11. Zhang, K., Merazga, Y., and Filbin, M. T. (1996) *J. Neurosci. Res.* **45,** 525–533
12. Brunden, K. R. (1992) *J. Neurochem.* **58,** 1659–1666
13. Sato, Y., Kimura, M., Yasuda, C., Nakano, Y., Tomita, M., Kobata, A., and Endo, T. (1999) *Glycobiology* **9,** 655–660
14. Jaques, A. J., Opdenakker, G., Rademacher, T. W., Dwek, R. A., and Zamze, S. E. (1996) *Biochem. J.* **316,** 427–437
15. Burger, D., Perruisseau, G., Simon, M., and Steck, A. J. (1990) *J. Neurochem.* **58,** 845–853
16. Burger, D., Perruisseau, G., Simon, M., and Steck, A. J. (1990) *J. Neurochem.* **58,** 854–861
17. Voshol, H., van Zuylen, C. W. E. M., Orberger, G., Vliegenthart, J. F. G., and Schachner, M. (1996) *J. Biol. Chem.* **271,** 22957–22960
18. Galustian, C., Lawson, A. M., Komba, S., Ishida, H., Kiso, M., and Feizi, T. (1997) *Biochem. Biophys. Res. Commun.* **240,** 748–751
19. Hardy, M. R., and Townsend, R. R. (1994) *Methods Enzymol.* **230,** 208–225
20. Kupce, E., Schmidt, P., Rabce, M., and Wagner, G. (1998) *J. Magn. Reson.* **135,** 361–367
21. Braunschweiler, L., and Ernst, R. R. (1983) *J. Magn. Reson.* **53,** 521–528
22. Bax, A., and Davis, D. G. (1985) *J. Magn. Reson.* **65,** 355–360
23. Griesinger, C., Otting, G., Wüthrich, K., and Ernst, R. R. (1988) *J. Am. Chem. Soc.* **110,** 7870–7872
24. Bax, A., and Davis, D. G. (1985) *J. Magn. Reson.* **63,** 207–213
25. Jeenerm, J., Meier, B. H., Bachmann, P., and Ernst, R. R. (1979) *J. Chem. Phys.* **71,** 4546–4553
26. Ciucanu, I., and Kerek, F. (1984) *Carbohydr. Res.* **131,** 209–217
27. Vorm, O., and Mann, M. (1994) *J. Am. Soc. Mass. Spectrom.* **5,** 955–958
28. Weisshaar, G., Hiyama, J., and Renwick, A. G. C. (1991) *Glycobiolgy* **1,** 393–404
29. Stroop, C. J. M., Weber, W., Nimtz, M., Gutiérrez Gallego, R., Kamerling, J. P., and Vliegenthart, J. F. G. (2000) *Arch. Biochem. Biophys.* **374,** 42–51
30. Vliegenthart, J. F. G., Dorland, L., and Van Halbeek, H. (1983) *Adv. Carbohydr. Chem. Biochem.* **41,** 209–374
31. De Waard, P., Koorevaar, A., Kamerling, J. P, and Vliegenthart, J. F. G. (1991) *J. Biol. Chem.* **266,** 4237–4243
32. Seppo, A., Pentilla, L., Leppanen, A., Maaheimo, H., Niemela, R., Helin, J., Wieruszeski, J.-M., and Rekonen, O. (1994) *Glycoconj. J.* **11,** 217–225
33. Dasgupta, S., Hogan, E. L., Glushka, J, and Van Halbeek, H. (1994) *Arch. Biochem. Biophys.* **310,** 373–384
34. Michalski, J. C., Wieruszeski, J.-M., Alonso, C., Cache, P., Montreuil, J., and Strecker, G. (1991) *Eur. J. Biochem.* **201,** 439–458
35. Dorland, L., Van Halbeek, H., Vliegenthart, J. F. G., Schaurer, R., and Wiegandt, H. (1986) *Carbohydr. Res.* **151,** 233–245
36. Michou, F., Brisson, J.-R., and Jennings, H. J. (1987) *Biochemistry* **26,** 8399–8405
37. Kitajima, K., Nomoto, H., Inoue, Y., Iwasaki, M., and Inoue, S. (1984) *Biochemistry* **23,** 310–316
38. Manzi, A., Salimath, P. V., Spiro, R. C., Keifer, P. A., and Freeze, H. H. (1995) *J. Biol. Chem.* **270,** 9154–9163
39. Gilbert, M., Brisson, J.-R., Karwaski, M.-F., Michniewicz, J., Cunningham, A.-M., Wu, Y., Young, N. M., and Wakarchuk, W. W. (2000) *J. Biol. Chem.* **275,** 3896–3906
40. Broberg, A., Thomsen, K. K., and Duus, J. Ø. (2000) *Carbohydr. Res.* **328,** 375–382
41. Schachner, M., Martini, R., Hall, H., and Orberger, G. (1995) *Prog. Brain Res.* **105,** 183–188
42. Schachner, M., and Martini, R. (1995) *Trends Neurosci.* **18,** 183–191
43. Hall, H., Lui, L., Schachner, M., and Schimtz, B. (1993) *Eur. J. Neurosci.* **5,** 34–42
44. Ilyas, A. A., Chou, D. K., Jungalwala, F. B., Costello, C., and Quarles, R. H. (1990) *J. Neurochem.* **55,** 594–601
45. Poduslo, J. F. (1990) *J. Biol. Chem.* **265,** 3719–3725
46. Mohan, P. S., Chou, D. K., and Jungalwala, F. B. (1990) *J. Neurochem.* **54,** 2024–2031
47. Bakker, H., Friedmann, I., Oka, S., Kawasaki, T., Nifant'ev, N., Schachner, M., and Mantei, N. (1997) *J. Biol. Chem.* **272,** 29942–29946
48. Ong, E., Yeh, J.-C., Ding, Y., Hindsgaul, O., and Fukuda, M. (1998) *J. Biol. Chem.* **273,** 5190–5195
49. Bistrup, A., Bhakta, S., Lee, J. K., Belov, Y. Y., Gunn, M. D., Zuo, F.-R., Huang, C.-C., Kannagi, R., Rosen, S. D., and Hemmerich, S. (1999) *J. Cell Biol.* **145,** 899–910
50. Lee, J. K., Bhakta, S., Rosen, S., and Hemmerich, S. (1999) *Biochem. Biophys. Res. Commun.* **263,** 543–549
51. Bowman, K. G., Hemmerich, S., Bhakta, S., Singer, M. S., Bistrup, A., Rosen, S. D., and Bertozzi, C. R. (1998) *Chem. Biol.* **5,** 447–460
52. Spiro, R. G., Yasumoto, Y., and Bhoyroo, V. (1996) *Biochem. J.* **319,** 209–216
53. Nastuk, M. A. Davis, S., Yancopoulos, G. D., and Fallon, J. R. (1998) *J. Neurosci.* **18,** 7167–7177
54. Uchimura, K., Maramatsu, H., Kadomatsu, K., Fan, Q.-W., Kurosawa, N., Mitsuoka, C., Kannagi, R., Habuci, O., and Maramatsu, T. (1998) *J. Biol. Chem.* **273,** 22577–22583
55. Noguchi, S. (1992) *Eur. J. Biochem.* **209,** 883–894
56. Kimura, N., Mitsuoka, C., Kanamori, A., Hhiraiwa, N., Uchimura, K., Muramatsu, T., Tamatani, T., Kansas, G. S., and Kannagi, R. (1999) *Proc. Natl. Acad. Sci. U. S. A.* **96,** 4530–4535
57. Needham, L. K., and Schnaar, R. L. (1993) *Proc. Natl. Acad. Sci. U. S. A.* **90,** 1359–1365
58. Kanda, T., Yamawaki, M., Ariga, T., and Yu, R. K. (1995) *Proc. Natl. Acad. Sci. U. S. A.* **92,** 7897–7901
59. Galili, U. (1993) *Springer Semin. Immunopathol.* **15,** 155–171
60. Thall, A. P., Maly, P., and Lowe, J. B. (1995) *J. Biol. Chem.* **270,** 21437–21440
61. Bergwerff, A. A., Stroop, C. J. M., Murray, B., Holtorf, A. P., Pluschke, G., van Oostrum, J., Kamerling, J. P., and Vliegenthart, J. F. G. (1995) *Glycoconj. J.* **12,** 318–330
62. Finne, J. (1975) *Biochim. Biophys. Acta* **412,** 317–325
63. Finne, J. (1989) *CIBA Found. Symp.* **145,** 173–183; discussion 183–188
64. Bouchon, B., Levery, S. B., Clausen, H., and Hakomori, S.-I. (1992) *Glycoconj. J.* **9,** 27–38
65. Finne, J. Krusius, T., and Rauvala, H. (1977) *Biochem. Biophys. Commun.* **74,** 405–410
66. Angata, K., Suzuki, M., McAuliffe, J., Ding, Y., Hindsgaul, O., and Fukuda, M. (2000) *J. Biol. Chem.* **275,** 18594–18601
67. Sato, C., Fukuoka, H., Ohta, K., Matsuda, T., Koshino, R., Kobayashi, K., Troy, F. A., and Kitajiama, K. (2000) *J. Biol. Chem.* **275,** 15422–15431
68. Georgiou, J., and Charlton, M. P. (1999) *Glia* **27,** 101–109
69. Griffith, L. S., Schmitz, B., and Schachner, M. (1992) *J. Neurosci. Res.* **33,** 639–648
70. Scheinder-Schaulies, J., Von Brunn, A., and Schachner, M. (1990) *J. Neurosci. Res.* **27,** 286–297
71. Filbin, M. T., and Tennekoon, G. I. (1991) *Neuron* **7,** 845–855
72. Hall, H., Vorherr, T., and Schachner, M. (1995) *Glycobiology* **5,** 435–441
73. Hall, H., Deutzmann, R., Timpl, R., Vaughan, L., Schimtz, B., and Schachner, M. (1997) *Eur. J. Biochem.* **246,** 233–242
74. Hall, H., Carbonetto, S., and Schachner, M. (1997) *J. Neurochem.* **68,** 544–553
75. Martini, R., Bollensen, E., and Schachner, M. (1988) *Dev. Biol.* **129,** 330–338
76. Martini, R., Xin, Y., Schmitz, B., and Schachner, M. (1992) *Eur. J. Neurosci.* **4,** 628–639
77. Martini, R., Xin, Y., and Schachner, M. (1994) *Glia* **10,** 70–74
78. McGarry, R. C., Helfland, S. L., Quarles, R. H., and Roder, J. C. (1983) *Nature* **306,** 376–378
79. Degrootte, S., Lo-Guidice, J.-M., Strecker, G., Ducourouble, M.-P., Roussel, P., and Lamblin, G. (1997) *J. Biol. Chem.* **272,** 29493–29501
80. Fan, Q.-W., Uchimura, K., Yuzawa, Y., Matsuo, S., Mitsuoka, C., Kannagi, R., Maramatsu, H., Kadomatsu, K., and Maramatsu, T. (1999) *Glycobiology* **9,** 947–955
81. Hiraoka, N., Petryniak, B., Nakayama, J., Tsuboi, S., Suzuki, M., Yeh, J.-C., Izawa, D., Tanaka, T., Miyasaka, M., Lowe, J. B., and Fukuda, M. (1999) *Immunity* **11,** 79–89
82. Finne, J., Krusius, T., Rauvala, H., and Hemminki, K. (1977) *Eur. J. Biochem.* **77,** 319–323
83. Kiang, W. K., Krusius, T., Finne, J., Margolis, R. U., and Margolis, R. K. (1982) *J. Biol. Chem.* **257,** 1651–1659
84. Fukuda, M., Dell, A., and Fukuda, M. N. (1984) *J. Biol. Chem.* **259,** 4782–4791
85. Fukuda, M., Lauffenburger, M., Sasaki, H., Rogers, M. E., and Dell, A. (1987) *J. Biol. Chem.* **262,** 11952–11957
86. Funakoshi, Y., Taguchi, T., Sato, C., Kitajima, K., Inoue, S., Morris, H. R., Dell, A., and Inuoe, Y. (1997) *Glycobiology* **7,** 195–205
87. Sato, C., Kitajima, K., Inoue, S., and Inoue, Y. (1998) *J. Biol. Chem.* **273,** 2575–2582
88. Sato, C., Inoue, S., Matsuda, T., and Kitajima, K. (1998) *Anal. Biochem.* **261,** 191–197